

Infrared Characterisation and Prediction of Aviation Turbine Fuel Plume

R. Nagarajan*, Karuna Poonia, S.D. Bilonia, and R. Singh

Defence Laboratory, Jodhpur – 342 011, India

**Email: r.nagarajan@dl.drdo.in*

ABSTRACT

Broad (3.7 μm - 4.8 μm) as well as narrow band (4.16 μm - 4.24 μm) mid wave infrared characterisation of plume has been reported here. Multiple angular measurements (azimuth) were carried out on a laboratory developed plume source with aviation turbine fuel (ATF) using thermal imaging systems. Correlation of IR prediction to experimental results is the key objectives of this study. As this narrow band covers the blue spike of plume, a comparison of the same with broad band plume contribution has been reported for the first time. Also, a model to simulate the IR radiation of two-dimensional parabolic jet was developed and used to predict spectral contribution from major hydrocarbon fuel combustion products (CO_2 and H_2O). In addition, it was found that the plume transmission characteristics extracted from imager measurements are qualitatively in agreement with prediction results.

Keywords: Thermal imager; Calibration; Plume; Aspect angle; IR signature and prediction

1. INTRODUCTION

The low observable technology for aircraft survivability has gained much concern due to increasing threat from heat seeking missiles. The IR signature estimation of aircrafts contributes in defining missile lock on range. The hot gaseous products from the combustion are one of the important IR radiation emitters along with various components such as hot engine parts and jet tail pipe. Since the availability of actual aircraft for infrared measurements as per requirement is less feasible and expensive, a cost effective scaled down laboratory plume source with mathematical model to characterise/predict the IR signature of the engine exhaust plume has been investigated in the present study. A code to predict plume radiation has also been developed in MATLAB and the results have been compared with the experimental data. The approach employed for the calculation is discussed thoroughly elsewhere¹. An in-house developed plume source which chemically mimics the jet engine exhaust has been used for IR measurement in (3.7 μm - 4.8 μm) band using MCT based thermal imager (Cedip, France).

There are considerable reported studies on experimental²⁻⁵ and computational investigations^{6,7} of IR signature analysis of plumes. It has been observed from the literature that infrared characterisation of plume has been carried out with either a spectral radiometer or a very narrow band filter, but no report is available to the best of author's knowledge about broad band measurement and its correlation to prediction results. Hence, an attempt is made to quantify the contribution of plume in broad band and narrow band (blue spike). Also, the experimental results are compared with prediction set. In addition, the

angular distribution of IR radiation with respect to sensor has been measured and compared with predicted results.

2. EXPERIMENTAL SET UP

The experimental setup used to generate the high temperature exhaust plumes is illustrated in Fig. 1. High pressure dry air rates at 125 cfm and ATF at 150 ml/min was supplied to the combustor liner. A portion of the air was used for convective cooling of the combustor liner. The convergent nozzle used here was designed with nozzle outlet diameters (D) as 5 cm. To estimate plume signature contribution and to correlate the theoretical prediction with measurement data, experiments were carried out in various sensor aspect angles. The measurements were carried out using dual integration time (IT) covering a temperature range of 330 $^{\circ}\text{C}$ – 1200 $^{\circ}\text{C}$.



Figure 1. Experimental setup.

3. THEORETICAL MODELLING

Need for modelling and measurements of infrared signature of exhaust plumes has increased with the increased risk of IR targeting missiles. Modelling of radiation emissions from exhaust jet is important and cost effective. The plume radiation is dominated by the radiation emitted from the plume core, which does not mix with the surrounding air and maintain the high temperature (T). Comparisons of measured and computed radiation intensities provide insights into the validity of calculations. The basic radiation heat transfer equation solved for the computation of radiation neglecting scattering is given by¹

$$\frac{dI_{\lambda}(s)}{ds} = -a_{\lambda}I_{\lambda}(s) + a_{\lambda}I_{\lambda B}(s) \quad (1)$$

$I_{\lambda}(s)$ is the radiance at position s , s is the localised distance, a_{λ} is absorption cross-section coefficient, $I_{\lambda B}$ is the blackbody radiation calculated by Planck's Law. The solution obtained by integrating Eqn. (1) can be written as Eqn. (2) given below

$$I_{\lambda}(s) = I_{\lambda}(s=0)\tau(o,s) + \int_0^s I_{\lambda B}(s')\frac{\partial}{\partial s'}\tau(s',s)ds' \quad (2)$$

The distribution of the physical properties such as plume temperature, density, mass fractions (CO_2 and H_2O) are numerically calculated by developing a MATLAB code based on the CFD module available as open source⁸. The calculation of plume transmission (τ) is based on the narrow band model and absorption cross-section data as explained⁹. $I_{\lambda}(s=0)$ is the initial radiation at $s=0$ which may be due to the radiation by any object behind plume. At certain aspect angles, the initial radiation is due to the nozzle interior also. The heat balance equation along with geometrical view factor calculated with unit sphere method has been solved for nozzle surface radiation.

4. RESULTS AND DISCUSSION

The IR contribution of ATF plume was assessed by both theoretically and experimentally using indigenously developed laboratory plume source. To avoid fluctuations due to transient effects, multiple frames (at least 1000 frames) were averaged and the resultant average data has been used for analysis. Also, the physical temperature of the plume at four different spots was measured using R-type thermocouple. A comparison of plume thermal profiles obtained in $4.16 \mu m - 4.24 \mu m$ and $3.7 \mu m - 4.8 \mu m$ is depicted in Fig. 2. The initial temperature hike and dip in first 15 pixels are due to the presence of thermocouple (for physical temperature measurement) placed at 2 cm away from nozzle exit along plume centre line.

Multiple experiments were carried to normalise the influence of reactant flow as well as environmental parameters. It was found through multiple experiments (performed on different days and timings) that there exists temperature variation in thermal profile, though the qualitative trend remains the same. It is observed from Fig. 2 that the measurement consistency in broad band is higher, though the broad band and narrowband measurements were carried out one after the other on day 1 and 2 for a fixed inlet flow parameters, sensor orientation, source-sensor distance, etc. Hence, the profile

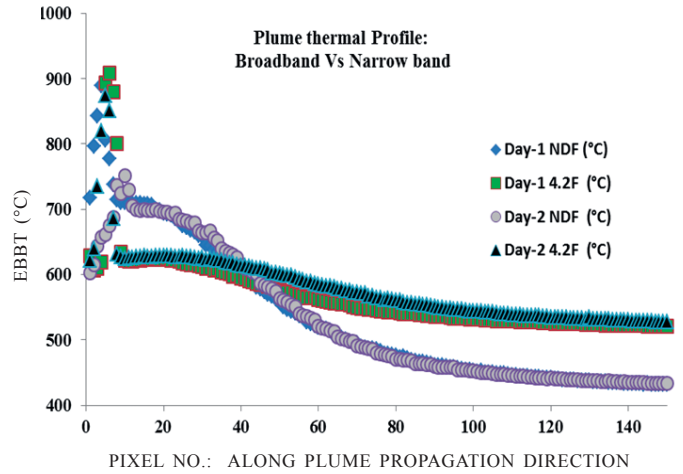


Figure 2. Thermal profile along plume axis in broad- and narrow-bands.

variation has some physical significance. The consistency of plume thermal profile for repeated measurements indicates the dominance of spectral behaviour. Since the narrow band measurement focuses only the CO_2 blue spike contribution around $4.2 \mu m$, contribution of the red spike ($\sim 4.4 \mu m$) is not taken into account. But, the dynamics of both the blue and red spikes were taken into account in broad band measurements. Hence, the variation in plume profile along the jet axis is well pronounced. On the other hand, as the broad band calibration accounts for black/grey body radiance distribution, error in intensity estimation due to the inclusion of non-emitting spectral wavelengths is inevitable. To reduce this calibration induced error, waveband selection in line with the emission band of the spectral source needs to be employed.

From the literature as well as preliminary measurements on ATF plume using spectral radiometer, it was understood that the plume spread is covered between $4.16 \mu m - 4.59 \mu m$. Hence, plume contribution in this band was determined based on experimental results. Theoretical prediction has also been done for plume contribution only in this waveband unless stated otherwise. The radiance plot thus obtained from experimental data has been plotted in Fig. 3. Since, radiance as measured by the camera is dependent on source temperature and emission

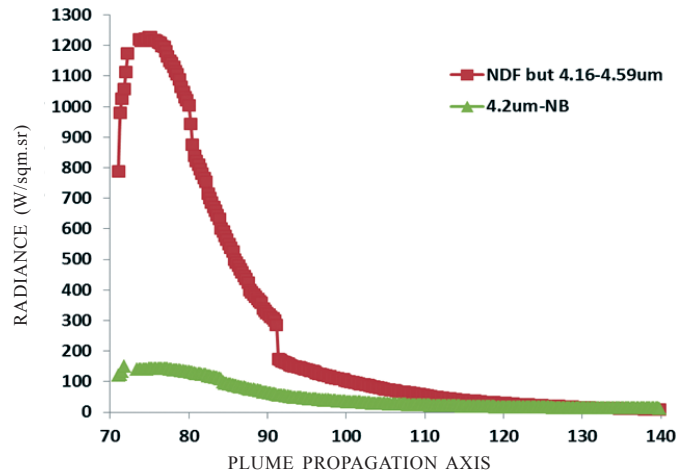


Figure 3. Plume radiance profile along plume axis in Narrow and broad bands.

characteristics, the radiance profile as shown in Fig. 3 follows similar pattern like thermal profile. However, apart from the source temperature and emissivity, the in-band radiance calculation is influenced by ambient as well as background temperature, etc.

The thermal images of plume captured using multiple integration time (IT) method has been shown in Fig. 4 for different aspect angles. As the nozzle interior is at high temperature, its contribution in addition to that of plume at certain aspect angles is expected. This in turn will define the distribution of radiation profile. As expected, the IR radiation received by the sensor at 0° aspect angle (in-line axis where the entire combustion chamber and nozzle interior can be seen visually) is higher due to the additional contribution of high temperature nozzle enclosure. There is no contribution of nozzle enclosure at broad side view (90°) and hence only the plume contribution is received at the sensor. This pattern is observed both in broad and narrow band experimental results. The physical temperature value measured by thermocouple (T_c) has been taken as reference for plume transmission calculations. As the T_c is placed at the middle of the plume, a complete transmission/attenuation in optical path depth of plume can be understood at least qualitatively. To estimate the optical depth attenuation, the transmission characteristics of the plume is adjusted by hit and trial method to achieve the mapped thermocouple temperature equal to that of T_c measured values. Table 1 shows the plume percent transmission values to bring T_c spot IR temperature equal to measured physical temperature (~1050 °C). From the table it is clear that the transmission in broad band is higher than that of narrow band, which implies higher attenuation in narrow band.

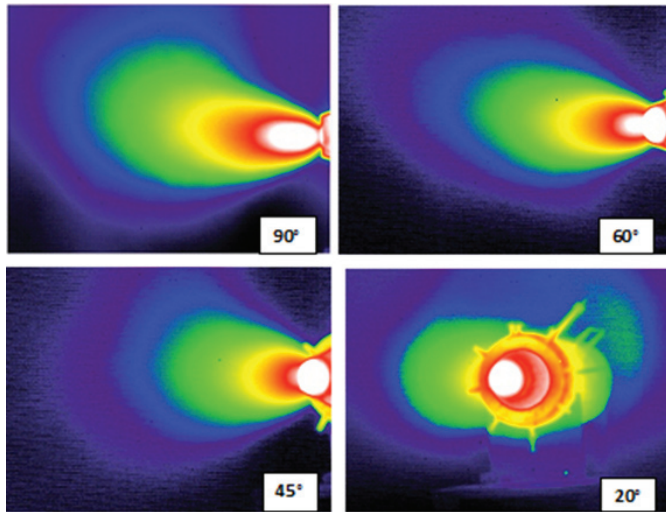


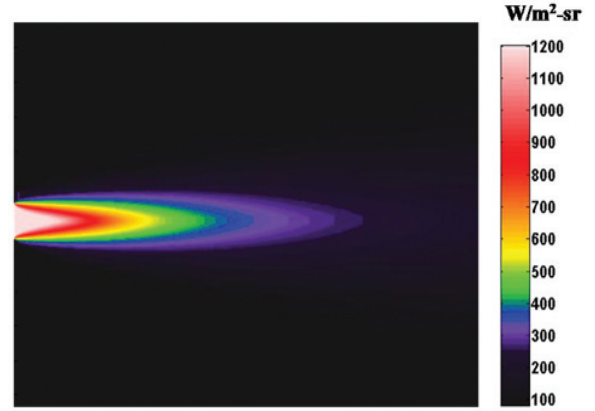
Figure 4. Thermal map of ATF plume in different aspect angles.

Figure 5 shows observed and predicted radiance profile of the plume. The theoretically developed plume profile does not cater the under expansion condition that was observed in experiments. This shows the limitations of numerical method used for CFD which cater the ideally expanded plume.

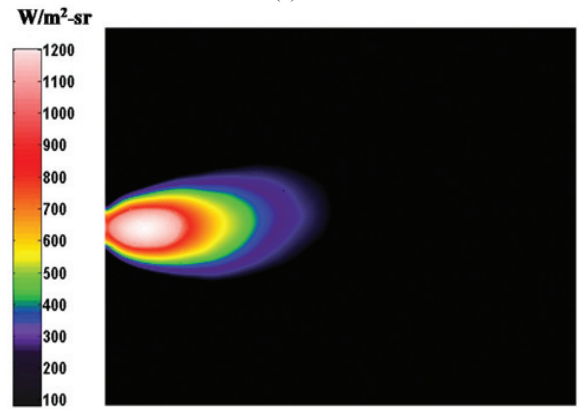
Figure 6 shows predicted spectral radiance at different axial distances from the nozzle exit along jet axis. The minor

Table 1. Plume transmission from IR mapped T_c spot

Emissivity		0.98			
		150 ml/min			
Fuel flow		Broad band		Narrow band	
Aspect angle		90°	0°	90°	0°
Through plume % transmission	Set-1	72.5	54.9	65.4	30.6
	Set-2	68	55.9	63.5	30.8



(a)



(b)

Figure 5. Comparison of the theoretically and experimentally obtained radiance profile: (a) Predicted and (b) Experimentally observed.

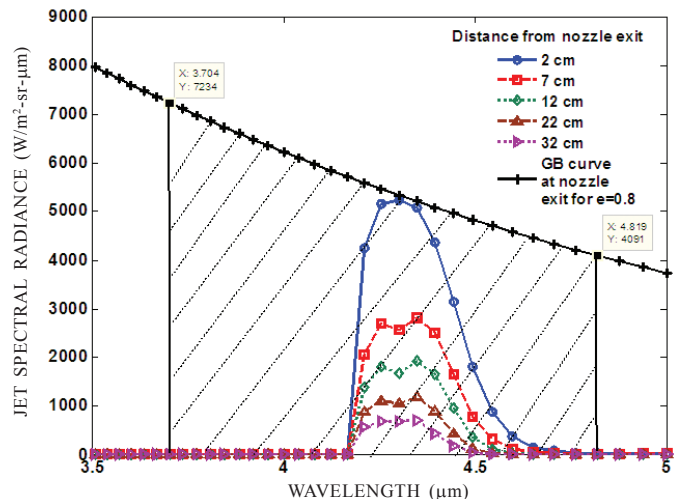


Figure 6. Spectral radiance behaviour along jet axis centre line.

dip around $4.3 \mu\text{m}$ is due to the heat flow from hot CO_2 region (core) to the cold CO_2 boundary. As it moves away from the nozzle exit both the concentration and the thermal contrast (between hot to cold region) decreased as shown in Fig 6. No atmospheric attenuation is taken into account for prediction.

Plume transmission along jet axis has also been predicted for both narrow and broad bands. It was observed that the plume transmission is increasing along axial distance as concentration and temperature decreasing with axial distance. The prediction trend is matching with experimental data. Figure 7 shows axial jet radiance distribution at different distances from the nozzle exit for three spectral bands $4.16 \mu\text{m} - 4.24 \mu\text{m}$, $4.16 \mu\text{m} - 4.59 \mu\text{m}$ and $3.7 \mu\text{m} - 4.8 \mu\text{m}$ (sensor limited). As expected, it is clear from Fig. 7 that radiance from broad band is higher than that of narrow band. The radiance in the plume core reduces sharply with distance for both the bands and after that the variation is gradual. The experimentally observed axial radiance distribution is shown in Fig. 3. After 5 cm of axial distance, the predicted radiance distribution is following the behaviour observed experimentally i.e., the radiance is decreasing with axial distance. The profile mismatch in first 5 cm from nozzle exit could be due to the formation of Mach disc and shock waves experienced in experiments. The predicted broad band and narrowband radiance distribution are in agreement with experimental results. The figure also shows that the emitted radiance calculated in the entire band $3.7 \mu\text{m} - 4.8 \mu\text{m}$ follows exactly the radiation profile of that in $4.16 \mu\text{m} - 4.59 \mu\text{m}$ band ensuring that the plume is emitting only in $4.16 \mu\text{m} - 4.59 \mu\text{m}$ wavelength band. It means that there is no IR contribution of jet emission in other mid infrared band except the wave band $4.16 \mu\text{m} - 4.59 \mu\text{m}$. This ensures the criteria of waveband selection for broad band measurements/analysis.

The angular distribution of plume radiance has been predicted for the same experimental conditions. Figures 8(a) and 8(b) shows the comparison of the predicted source radiance ($\text{W}/\text{m}^2\text{-sr}$) for various aspect angles with the experimental data in narrow band ($4.16 \mu\text{m} - 4.24 \mu\text{m}$) and broad band ($4.16 \mu\text{m} - 4.59 \mu\text{m}$), respectively (here 180° represents the plume in-line axis). The experimental results have been presented for

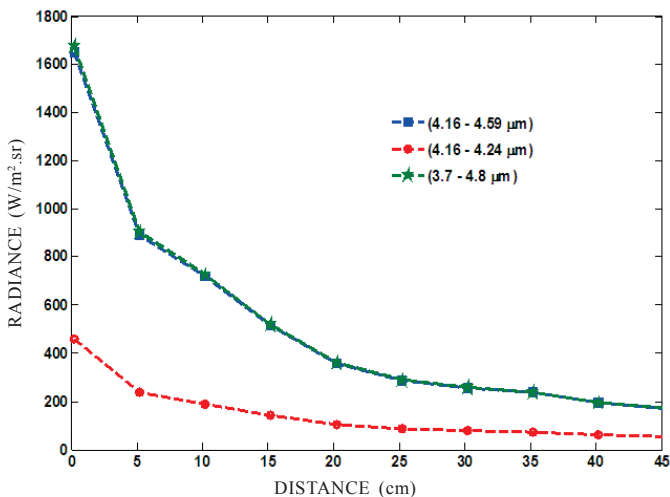


Figure 7. Axial radiance distribution along the axis centre line.

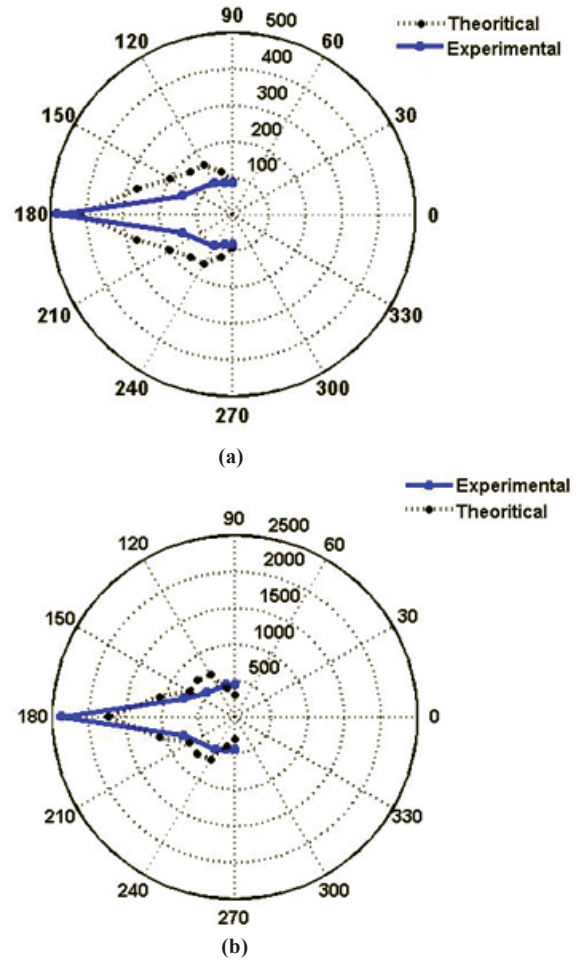


Figure 8. Angular distribution of predicted radiance vs experimental results: (a) Narrow band and (b) Broad band.

the plume area within the calibration range of the thermal imager; consequently a temperature cut off of 718 K is used for prediction. The experimental radiance along/around the plume axis is expected to be higher than predicted due to the fact that more of the nozzle outer surface with high temperature and emissivity is contributing to higher radiation along with plume which could not be accounted in the prediction. The correlation of theoretical results to the experimental one is very crucial. Practically, the plume emerging out of nozzle exit is diverging. Also, the hot core of plume is shifted to a few centimetres away from nozzle exit. This may be due to the under-expansion of jet (nozzle could not expand the flow to match the ambient condition at exit).

Also, there may be a possibility of incomplete combustion, which could result in presence of soot particles and some post combustion may occur which can shift the high temperature maxima away from nozzle exit. Such complex plume structure may possibly be handled through the advanced CFD tools. Emissivity correction is another challenge in bridging the predicted and experimental values of IR radiation. Application of multi-integration time and ‘gray body based calibration’ on measurement part and source with properly expanded jet will enhance validation.

5. CONCLUSIONS

The IR radiation of ATF plume using laboratory source has been estimated for narrow band (blue spike) as well as broad band (4.16 μm - 4.59 μm). Though the radiant intensity of plume is reported in literature for a narrow band (4.3 \pm 1 μm), an attempt to compare the contribution of blue spike and broad band has been reported here with prediction results. Also, from the experimental IR image and contact temperature measurement, a method is proposed to calculate plume transmission. The plume transmission thus obtained for narrow and broad bands are qualitatively in agreement with prediction results. Angular distribution of radiation has also been estimated experimentally and compared with prediction results.

REFERENCES

1. Heragu S.S. A Generalized model for infrared prediction from an engine exhaust. Indian Institute of Science, India, 1997 (PhD thesis).
2. Jellison G.P. & Miller D.P. Plume structure and dynamics from thermocouple and spectrometer measurements. *In Proceedings of SPIE*, 2006, **5425**, pp. 232-243. doi: 10.1117/12.542267
3. Blunck D.L. & Gore J.P. Study of narrowband radiation intensity measurements from subsonic exhaust plumes. *J. Prop. Pow.*, 2011, **27(1)**, 227-235. doi: 10.2514/1.47962
4. Haus, R.; Schafer, K.; Bautzer, W.; Heland, J.; Mosebach, H.; Bittner, H. & Eisenmann, T. Mobile fourier-transform infrared spectroscopy monitoring of air pollution. *App. Opt.*, 1994, **33**, 5682-5689. doi: 10.1364/AO.33.005682
5. Gross, L.A.; Griffiths, P.R. & Sun, J.N.-P. Temperature measurement by infrared spectroscopy. *In Infrared Methods for Gaseous Measurements*, Edited by J. Wormhoudt. Marcel Dekker Inc., New York, 1985, pp. 81-137.
6. Mahulikar, S.; Sonawane, H.; & Rao, A.; Infrared signature studies of aerospace vehicles. *Progress Aerospace Sci.*, 2007, **43(7-8)**, 218-245. doi: 10.1016/j.paerosci.2007.06.002
7. Jackson, H.T. An analytical model for predicting the radiation from jet plumes in the Mid-Infrared spectral region, US Army Report, April 1970.
8. www.fem.unicamp.br/~pheonics/SITE_PHOENICS/website/new/GENMIX/CODE.HTM (Accessed on 25 May 2015).
9. Ludwig, C.B.; Malkmus, W.; Freeman, G.N.; Slack, M. & Reed, R.A theoretical model for absorbing, emitting, and scattering plume radiation. *Spacecraft Radiative Transfer Temp. Control*, AIAA, 1982, **83**, 111-127.

ACKNOWLEDGEMENTS

The fund for this study has been granted from ADA for the project PIRSSA (ADA/AMCA/DLJ/IR/01/2011). The authors acknowledge the support and assistance of Mr Pabudan Singh and Mr Harimohan in entire experimental setup and data acquisition. Authors also acknowledge Dr S.S. Heragu for his technical discussion and guidance for theoretical prediction.

CONTRIBUTORS

Dr R. Nagarajan pursued his PhD in Infrared spectroscopy from the National Physical Laboratory (NPL), New Delhi /University of Delhi. He also worked as Associate Researcher at Oakland University, Rochester, MI, USA in Infrared micro spectroscopy of bio-materials. He is presently working as Scientist 'F' at Defence Laboratory, Jodhpur. His current area of research is Infrared camouflage/stealth aspects of airborne objects. In this study, he contributed in developing measurement methodology, supported in data acquisition, performed data analysis and drafted the manuscript.

Ms Karuna Poonia obtained her MSc (Physics) from University of Rajasthan, Jaipur in 2006. She has also obtained MTech in Opto Electronics & Optical Communication from Indian Institute of Technology (IIT), Delhi in 2010. She is presently working as Scientist 'B' at Defence Laboratory, Jodhpur. Her area of research is Infrared signature prediction. She is also involved in signature measurement and analysis of aircrafts. In this work, she contributed in IR prediction, supported in data acquisition and data analysis, performed data correlation between prediction and experiments; also she drafted the manuscript.

Mr Shambhu Dayal Bilonia received his BE (Mech.) from Govt. Engg. College, Ajmer in the year 2004. At present, he is working as Scientist 'D' at Defence Laboratory, Jodhpur. His present area of work is development of thermal target system and infrared signature studies related to aircrafts. In this present study, he contributed in design and development of plume source, performed partial data collection, and supported in drafting the manuscript.

Dr Ravindra Singh received his MTech (2001) and PhD (2008) from IIT Delhi. At present he is working as Scientist 'D' at Defence Laboratory, Jodhpur. His present area of research includes development of thermal target system and IR signature measurements of military platforms. In the present study, he contributed in performing experiments and data analysis, and supported in drafting the manuscript.